

SUPPLEMENTAL

We present in this supplementary material further details on the experimental procedures to generate the real-captured data-set, to measure reference frictional values and to render the synthetic data-set. We also include the raw friction values measured by the incline plane experiment and the corresponding prediction from our network.

S1 EXPERIMENTAL METHODS

S1.1 Details of Cloth Material

The details of cloth materials used in our experimental setup for capturing real test data are presented in Table S1. All materials, except silk, match the description of materials used and characterised by Wang et al. [33]. The equivalent class is also included in this table.




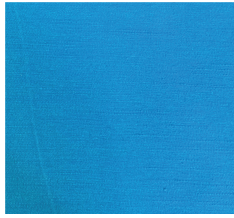



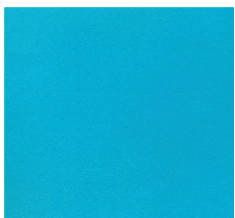
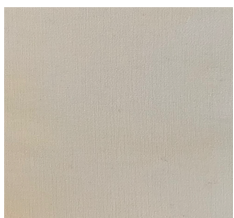
		
M01	M02	M03
Polyester 50% Rayon 50%	Polyester 95% Spandex 5%	Cotton 100%
0.187(Kg/m ³)	0.187(Kg/m ³)	0.75(Kg/m ³)
Camel Ponte Roma in [33]	Navy Sparkle Sweat in [33]	11oz Black Denim in [33]
		
M04	M05	M06
Cotton 65% Polyester 33% Spandex 2%	Polyester 100%	Polyester 100%
0.207(Kg/m ³)	0.198(Kg/m ³)	0.083(Kg/m ³)
Royal Target in [33]	Pink Ribbon Brown in [33]	Tango Red Jet Set in [33]
		
M07	M08	M09
Polyester 100%	Silk 100%	Cotton 95% Spandex 5%
0.150(Kg/m ³)	0.065(Kg/m ³)	0.268(Kg/m ³)
White Dots on Black in [33]	Not included in [33]	Ivory Rib Knit in [33]

TABLE S1
Experimental Cloth Materials

S1.2 Reference Friction Measurement

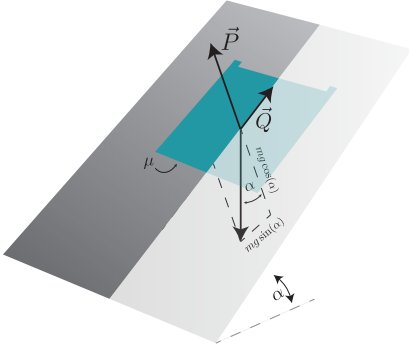


Fig. S1. Sketch of the inclined plane setup for frictional characterisation

In order to measure the reference friction coefficient for a material/substrate pair, we use the inclined plane protocol. As depicted in Figure S1, an object (with mass m , gravitational acceleration g) on an inclined plane, with angle of inclination α , is in equilibrium as long as the tangential part of its weight, $mg \sin(\alpha)$, is equal to the frictional force \vec{Q} and the normal part, $mg \cos(\alpha)$, is equal to the normal \vec{P} . As the angle α increases so does $mg \sin(\alpha)$. The mass m remains in equilibrium up to the limit where the frictional force reaches its maximum possible value $\vec{Q} = \mu \vec{P}$. This gives the relation for the friction coefficient $\mu = Q/P = \sin(\alpha)/\cos(\alpha) = \tan(\alpha)$.

For each substrate we test the angle at which a piece of cloth slides on it. From the angle we compute its tangent and we use this value as a friction coefficient. We test each piece of cloth on various parts of a substrate and do not find a noticeable difference in the slippage

angle.

Our measurements of friction coefficient are presented in results Tables starting from S2 in the 'Reference' columns, alongside predictions made by our model. Since our measurement is the angle of maximum inclination before sliding, and we move the inclined plane with a discrete interval of inclination angle $\delta\alpha$, the propagation of the error to the measured parameter $\mu = \tan(\alpha)$ is given by $\delta\mu \sim \pm \sec(\alpha)^2 \delta\alpha$.

S1.3 Drop and Drag Experiment

S1.3.1 Experimental Setup

The experimental setup consists in a rig of motorised stages Thorlabs holding a piece of cloth. The movement is followed by a led lamp to ensure consistent illumination. The drop and drag motion is captured from a well characterised view point. Two annotated views of the experimental setup for producing our real test data-set is presented in Figure S2.

S1.3.2 Motion Synchronisation

For our training with synthetic data to be meaningful, the experimental setup has to be accurate to a high degree, both in time and space. To this end we use two high precision Thorlabs motorised stages to control the vertical drop and the horizontal forth and back drag. We trigger a 5.0 MP Color Grasshopper3 Flir (former PointGrey) Camera at a frame rate of 2.4 frames/s, which gives a total of 300 frames for a full experiment. To match the experimental capture with the rendering of simulations we need to take into account the accelerations times and to be sure of the synchronisation between the camera and the motors. As described in the main manuscript, both motions were set to have an acceleration of 10 mm/s^2 until they reach a speed of 10 mm/s . The full movement is described by the vertical $z(t)$ and horizontal $x(t)$ positions:

	Drop		Drag
$z(t) = \begin{cases} \frac{at^2}{2} & \text{if } 0 < t \leq v/a \\ \frac{v^2}{2a} + vt & \text{if } v/a < t \leq T_1 - v/a \\ \frac{v^2}{2a} + vt - \frac{a}{2}(t - \frac{d_z}{v})^2 & \text{if } T_1 - v/a < t \leq T_1 \\ d_z & \text{if } T_1 < t \end{cases}$	$x(t) = \begin{cases} 0 & \text{if } 0 < t \leq T_1 \\ \frac{at^2}{2} & \text{if } T_1 < t \leq T_1 + v/a \\ \frac{v^2}{2a} + vt & \text{if } T_1 + v/a < t \leq T_2 - v/a \\ \frac{v^2}{2a} + vt - \frac{a}{2}(t - \frac{d_x}{v})^2 & \text{if } T_2 - v/a < t \leq T_2 \end{cases}$		

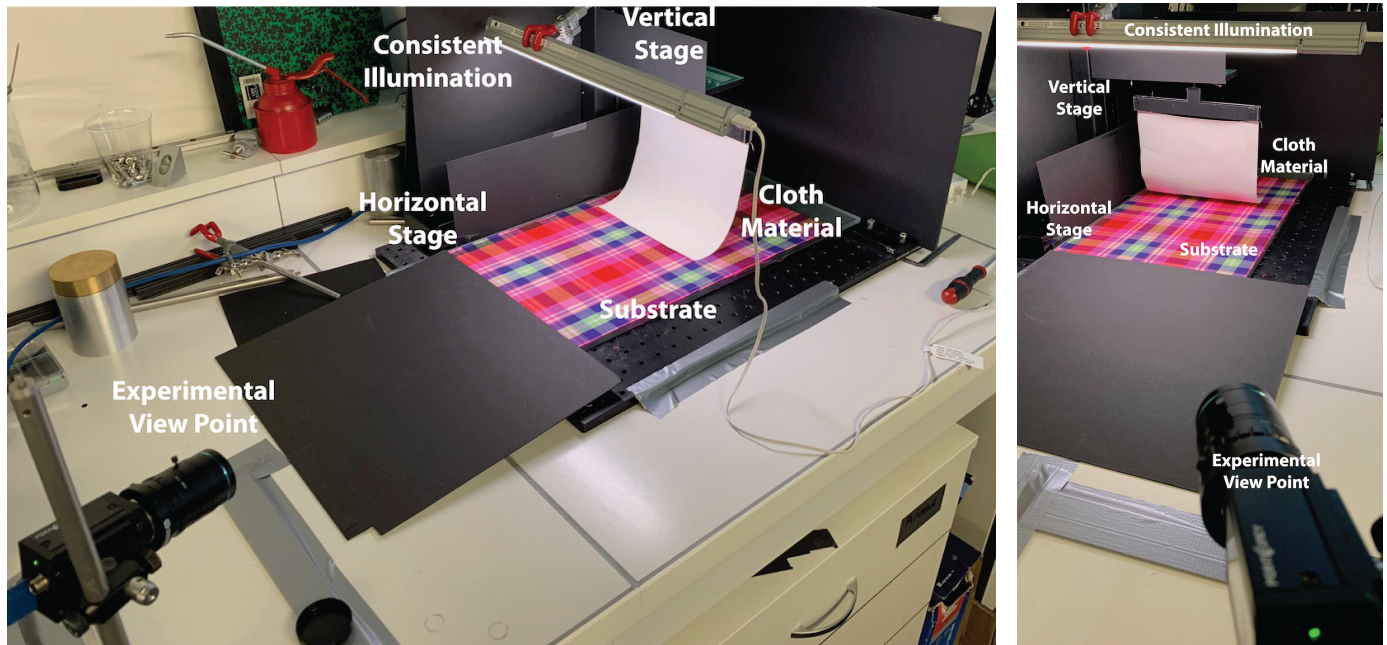


Fig. S2. Experimental setup for real data-set creation

where T_1, T_2, T_3, T_4 and T_f are computed accordingly from the corresponding displacements d_z and d_x .

Using the software drivers, we had access in real-time to the motor's position as well as the camera frame acquisition. In Figure S3 we show the good agreement between expected and measured positions as well as camera synchronisation.

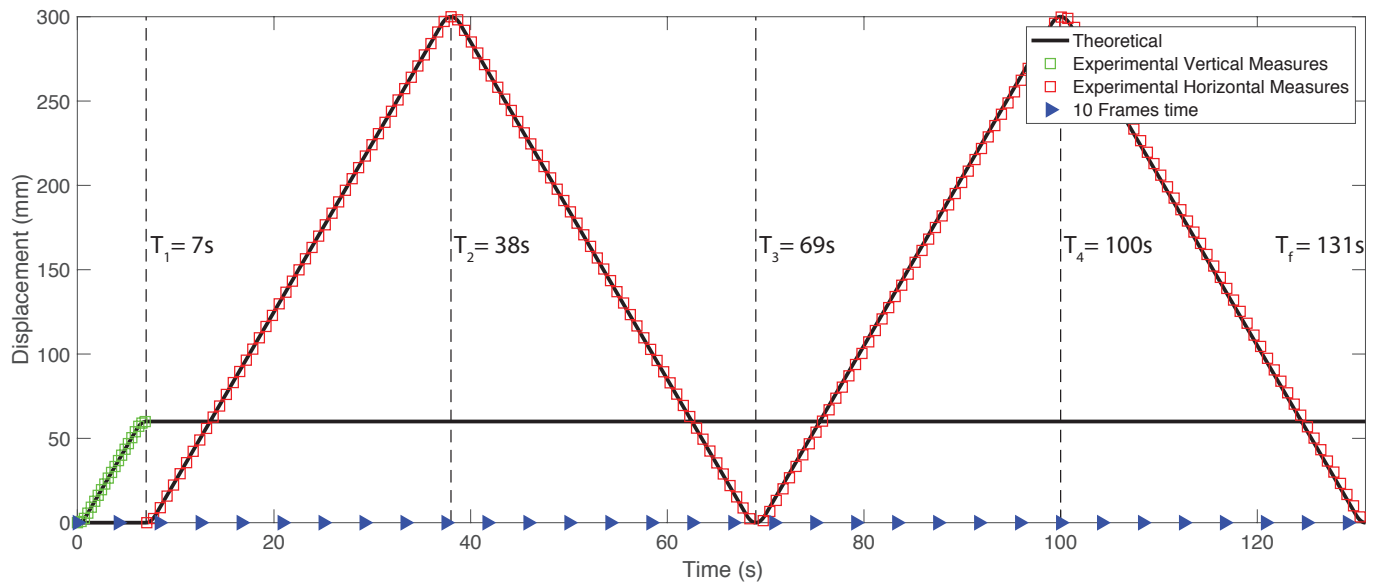


Fig. S3. Vertical and horizontal motors displacement for one complete drop and drag experiment

S1.3.3 Substrates selection and extension to Cloth materials

Friction is a complex phenomenon, that depends on the interfacial characteristics of the materials in contact at different scales. The selection of substrate is thus critical. To generate test data within the framework defined by Amontons-Coulomb's law we use different

hard substrates materials: Aluminium, Aluminium-PET, Ceramic, Rough Glass, Smooth Glass, Polyester, and Stainless. Experiments with such substrates are shown in Figure S4.

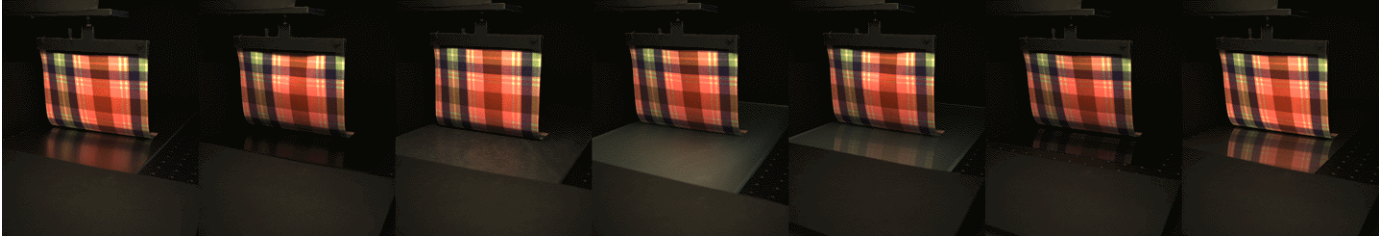


Fig. S4. Experimental images with various hard substrates for the same cloth material. From left to right: Aluminium, Aluminium-PET, Ceramic, Rough Glass, Smooth Glass, Polyester, and Stainless.

To test our network's capabilities with respect to more complex scenarios, that are not covered by Amontons-Coulomb's law, we extend our work to cloth-on-cloth friction, as shown in Figure .S5. To run these experiments, the textile material was slightly stretched and fixed on a hard substrate to avoid wrinkling. The reference measurement using the inclined plane setup was performed immediately before running the drop and drag experiment to capture the same state of the textile substrate.

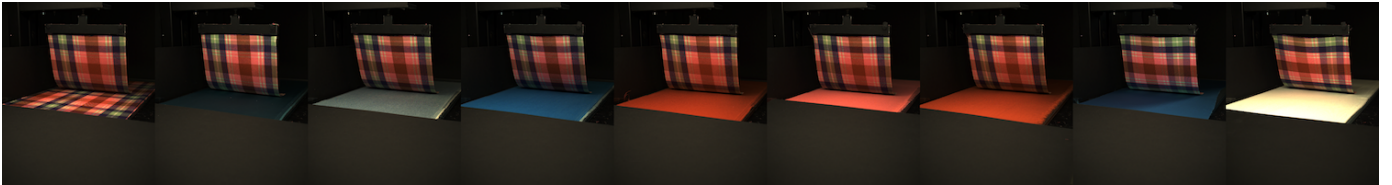


Fig. S5. Experimental images with different textile substrates for the same cloth material

S1.3.4 Rendering, Spatial calibration and reflectance

The synthetic images obtained with blender are rendered using the experimental camera parameters. We estimate those parameters by a standard camera calibration technique (pinhole model) and implemented a python based script that automates the rendering. We achieve a high degree of agreement as shown in Figure S6.

From Figure S4 we observe that some features are extremely important to improve the training process. In particular the inclusion of reflectance for the substrate is essential. In Figure S7 we show reflectance intensities used at random in our training process.

S2 DETAILED RESULTS FOR FRICTION BETWEEN CLOTH AND SUBSTRATE

The detailed results for our learning method on the prediction of static friction in cloth contact are presented in this section. In the following tables, accurate and inaccurate results have been marked by green and red colours respectively.

S2.1 Comparison between datasets

First we present the detailed results of the model's performance when it has been trained on synthetic datasets of varying accuracy. Table S2 presents results on training with Low-accurate-big-timestep and Table S3 shows results of training with High-accurate-small-timestep dataset. Finally, Table S4 presents predictions of friction coefficients by the model, when it has been trained on the dataset High-accurate-small-timestep. As illustrated by the number of green cells, the model trained on the most accurate dataset High-accurate-small-timestep performs the best on real test data. This comparison can be seen in Fig. 6.

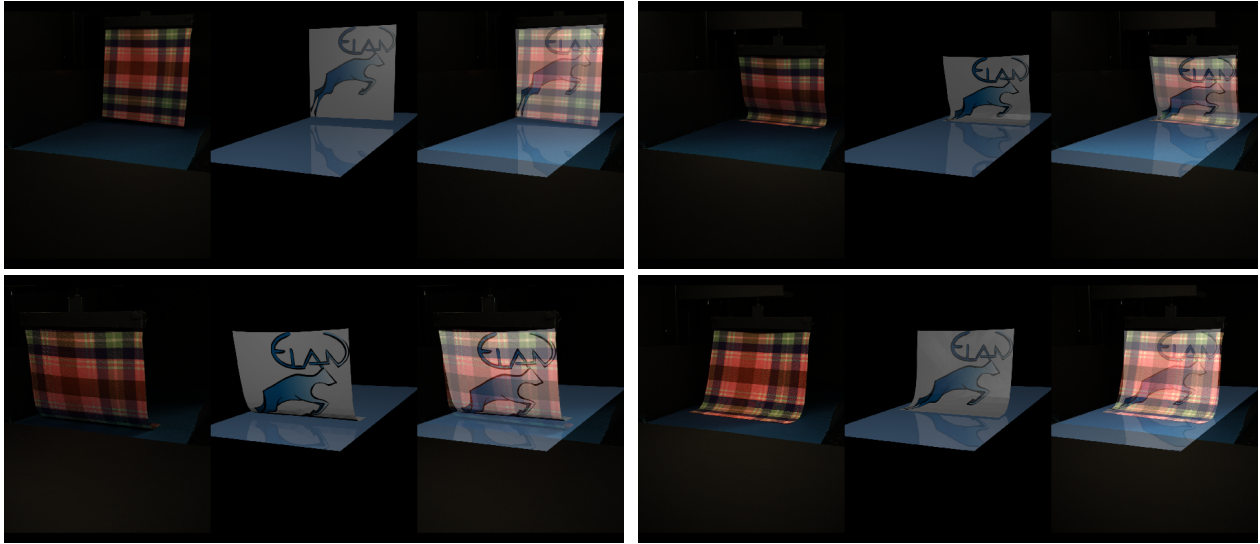


Fig. S6. Four instances of the drop and drag motion. Images on each panel correspond to: Experimental (left-most images), Rendered (center images), and Overlap (right-most images)

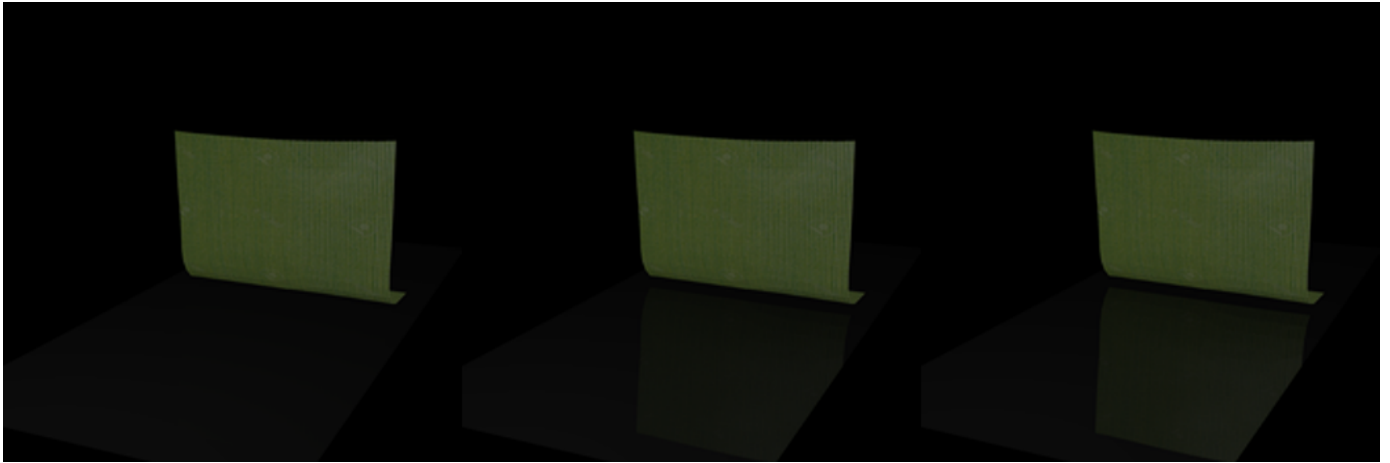


Fig. S7. The figure depicts multiple reflectance renderings on the substrate. The reflection of the green cloth can be seen in the substrate floor as the substrate is rendered with more reflectance

S2.2 Accuracy Improvement by Adding Rendering Variation

As discussed in Sec. 6.2, the results of training with High-accurate-small-timestep dataset presented in Table S4 represent training without varying the reflectance of the substrate during rendering (we plot the absolute error from the reference interval in red, black and light blue curves in Figure 7). It can be observed that the model gives fairly good results on substrates that are non-reflective in the real data *i.e.* Aluminium, Aluminium-PET, Ceramic, and Stainless. Table S5 presents the material predictions from our model, for this particular scenario.

Table S6 presents friction coefficient predictions when the model has been trained with data rendered with multiple reflectance values as presented in Figure S7. The results are shown in green curve in Figure 7, where we plot the absolute error from the reference interval. The results improve significantly on reflective substrates and also improve marginally on non-reflective substrates. Table S7 presents the material predictions for this scenario.

Substrate	Aluminium		Aluminium-PET		Ceramic		Glass-Rough	
Material	Reference	Predicted	Reference	Predicted	Reference	Predicted	Reference	Predicted
M01	0.47 ± 0.06	0.4	0.38 ± 0.06	0.0	0.45 ± 0.06	0.6	0.7 ± 0.08	0.9
M02	0.36 ± 0.06	0.0	0.42 ± 0.06	0.8	0.51 ± 0.07	0.8	0.55 ± 0.07	1.2
M03	0.51 ± 0.07	0.1	0.55 ± 0.07	0.2	0.62 ± 0.07	0.1	0.62 ± 0.07	0.2
M04	0.53 ± 0.07	1.0	0.51 ± 0.07	1.1	0.67 ± 0.08	1.0	0.62 ± 0.07	0.1
M05	0.34 ± 0.06	0.3	0.38 ± 0.06	0.5	0.42 ± 0.06	0.0	0.58 ± 0.07	1.3
M06	0.45 ± 0.06	0.6	0.51 ± 0.07	0.1	0.51 ± 0.07	0.2	0.49 ± 0.06	0.9
M07	0.58 ± 0.07	1.3	0.75 ± 0.08	0.9	0.78 ± 0.08	0.4	0.87 ± 0.09	0.1
M08	0.51 ± 0.07	0.6	0.7 ± 0.08	0.7	0.9 ± 0.09	1.0	0.87 ± 0.09	0.4
M09	0.45 ± 0.07	1.1	0.45 ± 0.06	0.2	0.55 ± 0.07	1.5	0.55 ± 0.07	0.9
Substrate	Glass-smooth		Polyester-mirror		Stainless			
Material	Reference	Predicted	Reference	Predicted	Reference	Predicted		
M01	0.38 ± 0.06	0.5	0.87 ± 0.09	1.2	0.55 ± 0.07	0.6		
M02	0.38 ± 0.06	0.4	1.07 ± 0.11	0.8	0.38 ± 0.06	1.3		
M03	0.34 ± 0.06	1.0	0.73 ± 0.08	0.5	0.3 ± 0.06	1.0		
M04	0.45 ± 0.06	0.4	0.7 ± 0.08	1.5	0.49 ± 0.06	1.3		
M05	0.36 ± 0.06	1.0	0.7 ± 0.08	0.5	0.38 ± 0.06	0.5		
M06	0.51 ± 0.07	1.4	1.04 ± 0.11	1.5	0.6 ± 0.07	1.2		
M07	1.15 ± 0.12	0.9	1.23 ± 0.13	0.7	0.75 ± 0.08	0.7		
M08	1.11 ± 0.12	0.4	1.04 ± 0.11	0.4	0.67 ± 0.08	0.8		
M09	0.38 ± 0.06	0.7	0.58 ± 0.07	0.2	0.4 ± 0.06	0.8		

TABLE S2
Friction predictions for real data with training on dataset Low-accurate-big-timestep

Substrate	Aluminium		Aluminium-PET		Ceramic		Glass-Rough	
Material	Reference	Predicted	Reference	Predicted	Reference	Predicted	Reference	Predicted
M01	0.47 ± 0.06	0.5	0.38 ± 0.06	0.4	0.45 ± 0.06	0.3	0.7 ± 0.08	1.1
M02	0.36 ± 0.06	1.3	0.42 ± 0.06	0.1	0.51 ± 0.07	0.6	0.55 ± 0.07	0.9
M03	0.51 ± 0.07	0.6	0.55 ± 0.07	0.8	0.62 ± 0.07	0.5	0.62 ± 0.07	1.0
M04	0.53 ± 0.07	0.3	0.51 ± 0.07	0.8	0.67 ± 0.08	0.2	0.62 ± 0.07	0.1
M05	0.34 ± 0.06	0.7	0.38 ± 0.06	0.7	0.42 ± 0.06	0.1	0.58 ± 0.07	0.2
M06	0.45 ± 0.06	0.7	0.51 ± 0.07	0.8	0.51 ± 0.07	0.2	0.49 ± 0.06	0.1
M07	0.58 ± 0.07	0.4	0.75 ± 0.08	0.7	0.78 ± 0.08	0.7	0.87 ± 0.09	0.2
M08	0.51 ± 0.07	0.1	0.7 ± 0.08	1.0	0.9 ± 0.09	0.7	0.87 ± 0.09	0.4
M09	0.45 ± 0.07	0.2	0.45 ± 0.06	0.6	0.55 ± 0.07	0.7	0.55 ± 0.07	0.4
Substrate	Glass-smooth		Polyester-mirror		Stainless			
Material	Reference	Predicted	Reference	Predicted	Reference	Predicted		
M01	0.38 ± 0.06	0.5	0.87 ± 0.09	0.5	0.55 ± 0.07	0.2		
M02	0.38 ± 0.06	0.5	1.07 ± 0.11	1.2	0.38 ± 0.06	0.7		
M03	0.34 ± 0.06	0.4	0.73 ± 0.08	0.4	0.45 ± 0.06	0.1		
M04	0.45 ± 0.06	0.7	0.7 ± 0.08	0.7	0.49 ± 0.06	0.3		
M05	0.36 ± 0.06	0.2	0.7 ± 0.08	0.3	0.38 ± 0.06	0.4		
M06	0.51 ± 0.07	0.4	1.04 ± 0.11	0.5	0.6 ± 0.07	0.5		
M07	1.15 ± 0.12	0.8	1.23 ± 0.13	0.6	0.75 ± 0.08	0.5		
M08	1.11 ± 0.12	0.8	1.04 ± 0.11	1.2	0.67 ± 0.08	0.5		
M09	0.38 ± 0.06	0.6	0.58 ± 0.07	1.0	0.4 ± 0.06	1.2		

TABLE S3
Friction predictions for real data with training on dataset Low-accurate-small-timestep

S3 DETAILED RESULTS FOR CLOTH ON CLOTH FRICTION

In this section we present the detailed results for cloth on cloth friction. The green cells in the following tables indicate accurate results within the error tolerance. The cells marked in yellow indicate predictions for baseline values that are outside the scope of the training data. As discussed in Sec. 7.3, Table S8 and Table S9 present results for cloth on cloth friction with and without fine-tuning on additional

Substrate	Aluminium		Aluminium-PET		Ceramic		Glass-Rough	
Material	Reference	Predicted	Reference	Predicted	Reference	Predicted	Reference	Predicted
M01	0.47 ± 0.06	0.5	0.38 ± 0.06	0.5	0.45 ± 0.06	0.5	0.7 ± 0.08	0.3
M02	0.36 ± 0.06	0.3	0.42 ± 0.06	0.3	0.51 ± 0.07	0.5	0.55 ± 0.07	0.1
M03	0.51 ± 0.07	0.5	0.55 ± 0.07	0.6	0.62 ± 0.07	0.6	0.62 ± 0.07	0.3
M04	0.53 ± 0.07	0.5	0.51 ± 0.07	0.5	0.67 ± 0.08	0.3	0.62 ± 0.07	0.2
M05	0.34 ± 0.06	0.4	0.38 ± 0.06	0.5	0.42 ± 0.06	0.4	0.58 ± 0.07	0.2
M06	0.45 ± 0.06	0.6	0.51 ± 0.07	0.5	0.51 ± 0.07	0.5	0.49 ± 0.06	0.3
M07	0.58 ± 0.07	0.5	0.75 ± 0.08	0.8	0.78 ± 0.08	0.5	0.87 ± 0.09	0.2
M08	0.51 ± 0.07	0.5	0.7 ± 0.08	0.7	0.9 ± 0.09	1.0	0.87 ± 0.09	0.6
M09	0.45 ± 0.07	0.9	0.45 ± 0.06	0.5	0.55 ± 0.07	0.5	0.55 ± 0.07	0.5

Substrate	Glass-smooth		Polyester-mirror		Stainless	
Material	Reference	Predicted	Reference	Predicted	Reference	Predicted
M01	0.38 ± 0.06	0.2	0.87 ± 0.09	1.0	0.55 ± 0.07	0.6
M02	0.38 ± 0.06	0.1	1.07 ± 0.11	0.6	0.38 ± 0.06	0.4
M03	0.34 ± 0.06	0.2	0.73 ± 0.08	0.5	0.45 ± 0.06	0.5
M04	0.45 ± 0.06	0.1	0.7 ± 0.08	0.7	0.49 ± 0.06	0.5
M05	0.36 ± 0.06	0.2	0.7 ± 0.08	0.6	0.38 ± 0.06	0.6
M06	0.51 ± 0.07	0.5	1.04 ± 0.11	0.6	0.6 ± 0.07	0.6
M07	1.15 ± 0.12	0.5	1.23 ± 0.13	0.6	0.75 ± 0.08	0.6
M08	1.11 ± 0.12	0.5	1.04 ± 0.11	0.5	0.67 ± 0.08	0.7
M09	0.38 ± 0.06	0.4	0.58 ± 0.07	0.8	0.4 ± 0.06	1.0

TABLE S4

Friction predictions for real data with training on dataset High-accurate-small-timestep

Material	Closest Class	Predicted Class
M1	Camel Ponte Roma	Royal Target
M2	Navy Sparkle Sweat	White Dots on Black
M3	11oz Black Denim	11oz Black Denim
M4	Royal Target	Royal Target
M5	Pink Ribbon Brown	White Dots on Black
M6	Tango Red Jet Set	Tango Red Jet Set
M7	White Dots on Black	White Dots on Black
M8	Not in Class (Silk)	Royal Target
M9	Ivory Rib Knit	Ivory Rib Knit

TABLE S5

Material predictions for real data with training on single reflectance rendering

rendered synthetic data respectively. Once the model has been fine-tuned on additional rendered data, it makes less catastrophic errors and the overall accuracy improves. These results have been presented in Fig. 11.

Substrate	Aluminium		Aluminium-PET		Ceramic		Glass-Rough	
	Reference	Predicted	Reference	Predicted	Reference	Predicted	Reference	Predicted
M1	0.47 ± 0.06	0.5	0.38 ± 0.06	0.4	0.45 ± 0.06	0.5	0.7 ± 0.08	0.6
M2	0.36 ± 0.06	0.3	0.42 ± 0.06	0.3	0.51 ± 0.07	0.5	0.55 ± 0.07	0.5
M3	0.51 ± 0.07	0.5	0.55 ± 0.07	0.6	0.62 ± 0.07	0.6	0.62 ± 0.07	0.7
M4	0.53 ± 0.07	0.5	0.51 ± 0.07	0.5	0.67 ± 0.08	0.4	0.62 ± 0.07	0.6
M5	0.34 ± 0.06	0.4	0.38 ± 0.06	0.5	0.42 ± 0.06	0.4	0.58 ± 0.07	0.5
M6	0.45 ± 0.06	0.6	0.51 ± 0.07	0.5	0.51 ± 0.07	0.5	0.49 ± 0.06	0.5
M7	0.58 ± 0.07	0.5	0.75 ± 0.08	0.8	0.78 ± 0.08	0.5	0.87 ± 0.09	0.6
M8	0.51 ± 0.07	0.5	0.7 ± 0.08	0.7	0.9 ± 0.09	0.7	0.87 ± 0.09	1.0
M9	0.45 ± 0.06	0.6	0.45 ± 0.06	0.5	0.55 ± 0.07	0.6	0.55 ± 0.07	0.5

Substrate	Glass-smooth		Polyester-mirror		Stainless	
	Reference	Predicted	Reference	Predicted	Reference	Predicted
M1	0.38 ± 0.06	0.4	0.87 ± 0.09	0.8	0.55 ± 0.07	0.6
M2	0.38 ± 0.06	0.3	1.07 ± 0.11	1.2	0.38 ± 0.06	0.4
M3	0.34 ± 0.06	0.3	0.73 ± 0.08	0.8	0.45 ± 0.06	0.5
M4	0.45 ± 0.06	0.5	0.7 ± 0.08	0.7	0.49 ± 0.06	0.5
M5	0.36 ± 0.06	0.5	0.7 ± 0.08	0.7	0.38 ± 0.06	0.5
M6	0.51 ± 0.07	0.5	1.04 ± 0.11	0.9	0.6 ± 0.07	0.6
M7	1.15 ± 0.12	1.2	1.23 ± 0.13	1.1	0.75 ± 0.08	0.8
M8	1.11 ± 0.12	0.9	1.04 ± 0.11	1.1	0.67 ± 0.08	0.7
M9	0.38 ± 0.06	0.4	0.58 ± 0.07	0.6	0.4 ± 0.06	0.5

TABLE S6

Friction predictions for real data with training on dataset High-accurate-small-timestep with multiple reflectance renderings

Material	Closest Class	Predicted Class
M1	Camel Ponte Roma	Royal Target
M2	Navy Sparkle Sweat	Navy Sparkle Sweat
M3	11oz Black Denim	11oz Black Denim
M4	Royal Target	Royal Target
M5	Pink Ribbon Brown	White Dots on Black
M6	Tango Red Jet Set	Tango Red Jet Set
M7	White Dots on Black	White Dots on Black
M8	Not in Class (Silk)	Royal Target
M9	Ivory Rib Knit	Ivory Rib Knit

TABLE S7

Material predictions for real data with training on multiple reflectance renderings

Cloth	M02		M05		M06		M07		M08	
	Ref.	Pred.	Ref.	Pred.	Ref.	Pred.	Ref.	Pred.	Ref.	Pred.
M01	0.6 ± 0.0712	1.3	1.96 ± 0.2535	1.2	2.48 ± 0.3744	1.1	2.36 ± 0.344	1.2	1 ± 0.1047	0.9
M02	0.21 ± 0.0547	0.4	0.62 ± 0.0725	0.7	0.7 ± 0.078	0.9	0.65 ± 0.0745	0.5	0.31 ± 0.0574	0.1
M03	0.9 ± 0.0948	1.1	8.14 ± 3.5217	1.5	2.75 ± 0.4483	1.1	2.14 ± 0.2921	0.6	1.04 ± 0.109	1.0
M04	0.81 ± 0.0867	0.7	1.73 ± 0.2091	1.3	2.36 ± 0.344	1.2	1.23 ± 0.1316	1.0	0.84 ± 0.0893	0.6
M05	0.25 ± 0.0556	0.6	1.54 ± 0.1765	1.1	1.38 ± 0.1521	1.1	1.04 ± 0.109	1.1	0.42 ± 0.0616	0.6
M06	0.32 ± 0.0577	0.3	0.67 ± 0.0759	1.0	0.78 ± 0.0842	0.7	0.9 ± 0.0948	0.7	0.47 ± 0.0639	0.3
M07	0.4 ± 0.0607	0.9	4.7 ± 1.209	1.3	1.48 ± 0.167	1.5	1.33 ± 0.145	1.1	0.53 ± 0.0671	0.9
M08	0.6 ± 0.0712	0.3	1.43 ± 0.1594	1.2	1.33 ± 0.145	0.5	1.33 ± 0.145	1.0	0.93 ± 0.0976	0.3
M10	0.51 ± 0.066	0.5	4.33 ± 1.034	1.3	2.05 ± 0.2724	1.1	2.36 ± 0.344	1.1	0.78 ± 0.0842	0.7

TABLE S8

Friction predictions for Cloth on Cloth real data, without fine tuning.

Cloth	M02		M05		M06		M07		M08	
	Ref.	Pred.	Ref.	Pred.	Ref.	Pred.	Ref.	Pred.	Ref.	Pred.
M01	0.6 ± 0.0712	0.6	1.96 ± 0.2535	1.4	2.48 ± 0.3744	0.9	2.36 ± 0.344	1.5	1 ± 0.1047	1.2
M02	0.21 ± 0.0547	0.3	0.62 ± 0.0725	0.6	0.7 ± 0.078	0.6	0.65 ± 0.0745	0.7	0.31 ± 0.0574	0.4
M03	0.9 ± 0.0948	0.8	8.14 ± 3.5217	1.5	2.75 ± 0.4483	1.0	2.14 ± 0.2921	1.3	1.04 ± 0.109	1.1
M04	0.81 ± 0.0867	0.7	1.73 ± 0.2091	1.4	2.36 ± 0.344	1.4	1.23 ± 0.1316	1.3	0.84 ± 0.0893	0.8
M05	0.25 ± 0.0556	0.4	1.54 ± 0.1765	1.4	1.38 ± 0.1521	0.9	1.04 ± 0.109	1.0	0.42 ± 0.0616	0.5
M06	0.32 ± 0.0577	0.4	0.67 ± 0.0759	0.7	0.78 ± 0.0842	0.7	0.9 ± 0.0948	1.1	0.47 ± 0.0639	0.3
M07	0.4 ± 0.0607	0.6	4.7 ± 1.209	1.3	1.48 ± 0.167	1.4	1.33 ± 0.145	0.9	0.53 ± 0.0671	0.6
M08	0.6 ± 0.0712	0.8	1.43 ± 0.1594	0.8	1.33 ± 0.145	0.6	1.33 ± 0.145	1.2	0.93 ± 0.0976	0.7
M10	0.51 ± 0.066	0.5	4.33 ± 1.034	1.4	2.05 ± 0.2724	1.4	2.36 ± 0.344	1.5	0.78 ± 0.0842	0.7

TABLE S9

Friction predictions for Cloth on Cloth real data, with fine tuning.